Part II. Heat Transfer

JOHN D. GABOR, BRUCE E. STANGELAND, and WILLIAM J. MECHAM
Argonne National Laboratory, Argonne, Illinois

Effective thermal conductivities for lateral heat transfer were measured in a fluidized-packed bed. An analysis of the mechanism of heat transfer was made by comparison with previously determined rates of solids mixing. A general correlation was made of the fluidized-packed bed thermal diffusivities with the size of the fixed packing and the minimum fluidization velocity in a manner similar to the correlation for lateral solids mixing diffusivities in a fluidized-packed bed.

Although the high heat transfer rates in a fluidized bed are attributed to convective transport by the fluidized particles, no direct comparison has been made between rates of heat transfer and rates of solids mixing. In order to obtain further understanding of the mechanisms of fluidized particle heat transfer, thermal conductivity measurements were made in a rectangular column of the same size used for the solids mixing studies described previously (Part I).

There are little basic thermal conductivity data available for fluidized-packed beds. Ziegler and Brazelton (*4*) made a systematic study of fluidized-packed bed heat transfer with various combinations of fixed packing and fluidized particle sizes for low gas velocities ($<$ 0.25 ft./sec.). Gabor and Stangeland (*3*) determined thermal conductivities in the longitudinal (axial) direction, and Bayens (*1*) made several measurements of thermal conductivities in the lateral (radial) direction. Frischmuth (*2*) made some measurements to determine the effect of fixed packing thermal conductivity on the radial thermal conductivity of a fluidized-packed bed. In this paper a comparison is made between lateral fluidized particle mixing and lateral heat transfer. The thermal diffusivities are then correlated in a manner similar to the solids mixing diffusivities.

EXPERIMENTAL

The rectangular column used in this study was 1 11/16 in. wide by 8½ in. high by 7 in. long (shown in Figure 1). The two ends were aluminum plates to which copper cooling coils were bonded to the external surface with a plastic heat transfer cement. The two long sides of the column were ½ in. thick transparent plastic, Plexiglas, to which the cooling plates were bolted and cemented. The gas distributor was a sintered stainless steel plate. Water was supplied to the cooling coils by a constant head tank, and the flow was measured by collection in a graduated cylinder during known time intervals. Water inlet and outlet temperatures were monitored by iron-constantan thermocouples. The fluidizing gas flow was measured by a rotameter.

The heater was an electrical resistance bayonet heater 6 in. long, 1½ in. wide, and ⅛ in. thick. Current was supplied and regulated by a variable auto transformer. Power input was measured by a voltmeter and ammeter. An iron-constantan thermocouple was spot welded to one side of the heater to measure heater skin temperatures.

Bruce E. Stangeland is with the University of California, Berkeley, California.

Bed temperature probes were made by drilling holes into the steel balls used for the bed packing and soldering the thermocouple ends inside the holes. Three or four probes were placed at heights of 3 or 6 in. on each side of the heater which was located in the center of the column. Because of the larger thermal conductivity in the vertical direction compared with the horizontal direction, the temperatures were essentially uniform in vertical cross section.

The packed-bed height for all runs was 6 in. Packing consisted of ½-, ⅜-, ¼-, and ⅛-in. steel spheres. For each run the amount of fluidized particles was adjusted so that the height of the fluidized bed was also 6 in. If the fluidized portion of the bed were less than 6 in., the 6-in. heater would not have transferred all its heat through a fluidized-packed bed; if the fluidized particles extended above the packing, the heat transfer rates would have been somewhat higher because of the freer movement of the particles above the restrictions of the packing.

One series of runs was made with helium as a fluidizing gas. All other runs used air. Table 1 lists the fluidizing materials and the fluidization and physical properties for the systems studied.

For the case of a constant cross-sectional area the Fourier equation relating rate of heat transfer to thermal conductivity can be integrated to

$$q = k A \frac{\Delta t}{\Delta x} \tag{1}$$

The lateral temperature profiles were generally linear, and therefore the effect of heat losses to the gas stream and to the

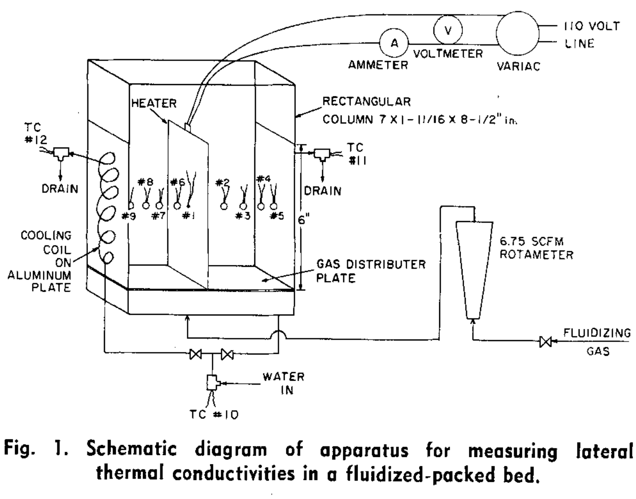

Fig. 1. Schematic diagram of apparatus for measuring lateral thermal conductivities in a fluidized-packed bed.

TABLE 1. FLUIDIZATION AND PHYSICAL PROPERTIES OF FLUIDIZED-PACKED BED SYSTEMS USED IN LATERAL HEAT TRANSFER STUDIES

Fluidized material	Fluidized particle size mesh	Packing diameter, in.	Fluidizing gas	V_{mf}, ft./sec.	Particle density, ρ, lb./cu. ft.	Particle C_p, B.t.u./(lb.)(°F.)
Cu-Ni	−140 + 170	⅜	Air	0.12	555	0.105
Cu-Ni	−140 + 170	⅜	Helium	0.28	555	0.105
Cu-Ni	−100 + 120	½	Air	0.28	555	0.105
Cu-Ni	−100 + 120	⅜	Air	0.28	555	0.105
Cu-Ni	−100 + 120	¼	Air	0.28	555	0.105
Cu-Ni	−100 + 120	⅛	Air	0.28	555	0.105
Cu-Ni	−60 + 70	¼	Air	0.71	555	0.105
Cu-Ni	−40 + 50	⅜	Air	1.56	555	0.105
Cu-Ni	−40 + 50	¼	Air	1.56	555	0.105
Alumina	−60 + 70	⅜	Air	0.36	249	0.217
Glass	−40 + 50	⅜	Air	0.39	137	0.20

ambient air through the column walls could be assumed small. The effective bed thermal conductivities were based on the average of the temperature gradients on both sides of the centrally located heater. The heat flux q was based on the heat pickup of the water in the cooling coils.

DISCUSSION OF RESULTS

Since the heat is transported through the bed by the moving fluidized particles, the experimental results are expressed in terms of thermal diffusivity. The thermal diffusivity α is related to the effective bed thermal conductivity k_e by

$$\alpha = \frac{k_e}{\rho_B C_p} \tag{2}$$

The fluidized (expanded) bed density ρ_B is based on the total weight of fluidized particles divided by the volume of the bed uncorrected for the void fraction of the fixed packing. The packing dilutes the amount of particles, and hence the reduction of heat carrying capacity of the particles must be compensated for by including the volume occupied by the fixed packing.

One set of runs was made with ⅜-in. diameter Lucite spheres to determine the effect of packing material on α. There was essentially no difference between the value of α for the Lucite packed bed and the steel packed bed, although there is about a factor of 50 difference in the thermal conductivities of the two materials. This result is confirmed by Frischmuth (2) who found that packings of glass, steel, and copper spheres all yield the same heat transfer properties. Therefore, it is concluded that the heat is essentially all transported by the moving fluidized particles.

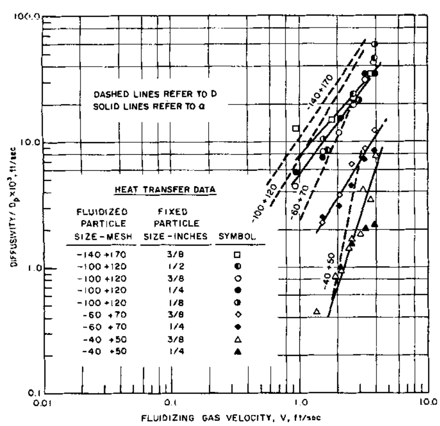

Fig. 2. Comparison of solids mixing diffusivities with thermal diffusivities for copper-nickel shot fluidized in the voids of fixed spherical packing.

Since the heat is transported by the moving fluidized particles, it would be expected that the thermal diffusivity and the solids mixing diffusivity would be related. On Figure 2 the thermal diffusivities α for the copper-nickel shot are compared with the solids mixing diffusivities D. The gas velocity is based on room temperature and pressure. The slight increase in velocity because of increase in gas temperature in the heated bed (average bed temperature about 50°C) was neglected. Because the lateral motion of the particles depends upon the amount of deflection by the fixed packing, the diffusivities were divided by the fixed packing diameter D_p. The experimental points for the thermal diffusivities are shown. The dashed lines represent the mixing diffusivities. For each different particle size the α's are less than the D's by about a factor of 2. This can be accounted for in that the fluidized particles do not come to an equilibrium temperature immediately with their surroundings as they move from one point of the bed to another. Although the rate of particle movement is the same for both the heat transfer and mixing studies because of the time lag in transfer of sensible heat by the fluidized particles, there results a reduced rate of heat transfer. Since the heat transfer is essentially effected by transport of the fluidized solids, the rate of heat transfer can be expressed in terms of the rate of solids mixing:

$$q = -Q\,D\,A\,\frac{dC}{dx} \tag{3}$$

The above term Q is the sensible heat released by the fluidized particles as they move to different points in the fluidized-packed bed. Since the tracer for the particle concentration change in a system in which heat transfer is being measured is temperature, the concentration gradient can be expressed in terms of a temperature gradient and combined with Q, the sensible heat transferred, expressed in terms of particle heat capacity and particle temperature change:

$$q = -\frac{(T_1 - T_2)}{(T_1 - T_s)}\,C_p\,\rho_B\,D\,A\,\frac{dT_s}{dx} \tag{4}$$

The term $(T_1 - T_2)/(T_1 - T_s)$ represents the fraction actually transferred of the total heat content that could thermodynamically be transferred by the particles as they change surroundings. It then follows from the Fourier equation that

$$k_e\,A\,\frac{dT_s}{dx} = \frac{(T_1 - T_2)}{(T_1 - T_s)}\,C_p\,\rho_B\,D\,A\,\frac{dT_s}{dx} \tag{5}$$

$$\frac{(T_1 - T_2)}{(T_1 - T_s)}\,D = \frac{k_e}{\rho_B C_p} = \alpha \tag{6}$$

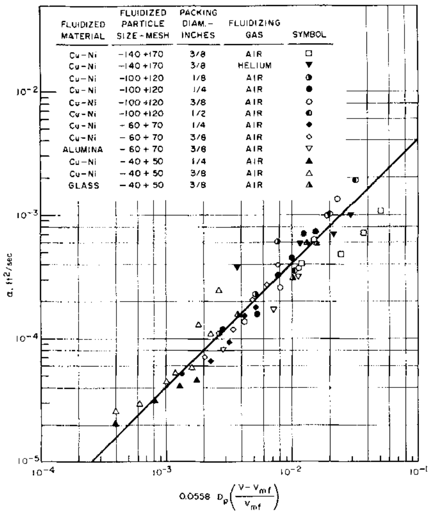

Fig. 3. General correlation of thermal diffusivities for lateral heat transfer in a fluidized-packed bed.

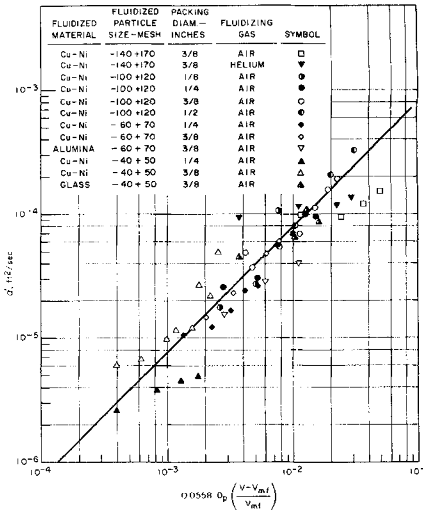

Fig. 4. General correlation of thermal diffusivities based on fluidized particle density for lateral heat transfer in a fluidized-packed bed.

If the particles were to reach equilibrium, the term $(T_1 - T_2)/(T_1 - T_s)$ would be 1. However, because the particles move from point to point before they attain the temperatures of the surroundings, α is less than D. It should be noted from Figure 2 that at the lower gas velocities the thermal diffusivities approach the values of the solids mixing diffusivities. At the lower gas velocities the particle motion is less, a circumstance which results in a longer residence time for the particles to reach equilibrium.

Since the mechanism of heat transfer is the same as that of particle mixing except for the added factor of slow heat release from particles, it would follow that the thermal diffusivities could be correlated in the same fashion as the mixing diffusivities. In Part I a general correlation was developed for relating the solids mixing with the basic parameters of fixed packing size, minimum fluidization velocity, and fluidizing gas velocity. On Figure 3 is a correlation of thermal diffusivity with 0.0558 D_p $(V - V_{mf})/V_{mf}$. Again the slope of the curve is unity, and other materials besides copper-nickel shot are included which gives support to the theoretical mechanism proposed in Part I.

The correlation can be expressed as

$$\frac{k_e}{\rho_B C_p} = \alpha = (0.04)\ 0.0558\, D_p \left[\frac{V - V_{mf}}{V_{mf}}\right] \quad (7)$$

All units are in feet and seconds.

However, of more value for engineering calculations is the thermal conductivity of the bed rather than the thermal diffusivity. The thermal conductivity can be determined from the above correlation if the density of the fluidized bed is known. This density is a function of the bed expansion. At present there is no good means for predicting bed expansion for gas fluidized beds, whereas minimum fluidization velocities can be predicted quite well. Therefore, a modified thermal diffusivity α' based on the density of the fluidized particle rather than the density of the bed was plotted vs. 0.0558 D_p $(V - V_{mf})/V_{mf}$ (see Figure 4). This correlation neglects change in fluidized bed density. The scatter is just slightly more than for the correlation for thermal diffusivity on Figure 3. The correlation on Figure 4 permits an estimation of thermal conductivity from the minimum fluidization velocity and the size of the fixed packing. The correlation on Figure 4 can be expressed as

$$\frac{k_e}{\rho C_p} = \alpha' = (0.0075)\ 0.0558\, D_p \left[\frac{V - V_{mf}}{V_{mf}}\right] \quad (8)$$

All units are in feet and seconds.

NOTATION

- A = cross-sectional area, sq. ft.
- C = concentration, lb./cu. ft.
- C_p = heat capacity, B.t.u./lb. °F.
- D = mixing diffusivity, sq. ft./sec.
- D_p = fixed packing diameter, ft.
- k = thermal conductivity, B.t.u./(hr.)(sq. ft.)(°F./ft.)
- k_e = effective bed thermal conductivity, B.t.u./(hr.)(sq. ft.)(°F./ft.)
- q = rate of heat transfer, B.t.u./hr.
- Q = sensible heat released from particle, B.t.u./lb.
- t = temperature, °F.
- T_s = temperature of surroundings, °F.
- T_1 = initial temperature of particle, °F.
- T_2 = final temperature of particle, °F.
- V = fluidizing gas velocity corrected for fixed packing voidage, ft./sec.
- V_{mf} = minimum fluidization gas velocity corrected for fixed packing voidage, ft./sec.
- x = distance, ft.
- α = thermal diffusivity, sq. ft./sec.
- α' = thermal diffusivity based on ρ, sq. ft./sec.
- ρ = density of fluidized particle, lb./cu. ft.
- ρ_B = fluidized bed density, lb./cu. ft.

LITERATURE CITED

1. Bayens, Charles, Argonne National Laboratory, Chemical Engineering Division Summary Report, *ANL-6333*, p. 178 (January, February, March, 1961).
2. Frischmuth, R. W., M.S. thesis, Northwestern University, Evanston, Illinois (1963).
3. Gabor, J. D., and B. E. Stangeland, Argonne National Laboratory, Chemical Engineering Division Summary Report, *ANL-6648*, p. 148 (October, November, December, 1962).
4. Ziegler, E. N., and W. T. Brazelton, *Ind. Eng. Chem. Process Design and Development*, **2**, No. 4, p. 276 (1963).

Manuscript received April 13, 1964; revision received August 7, 1964; paper accepted August 16, 1964.